

One-Step Process for Multi-gradient Wettability Modification on a PDMS Surface

Xinxin Li^{a,1}, Xinyu Mao^{a,1}, Xudong Li¹, Chong Liu^{*a}, Jingmin Li^{*a}

^a Department of Mechanical Engineering, Dalian University of Technology, Dalian, Liaoning, China

* Correspondence, E-mail: chongl@dlut.edu.cn; jingminl@dlut.edu.cn

¹ These authors contributed equally to this work

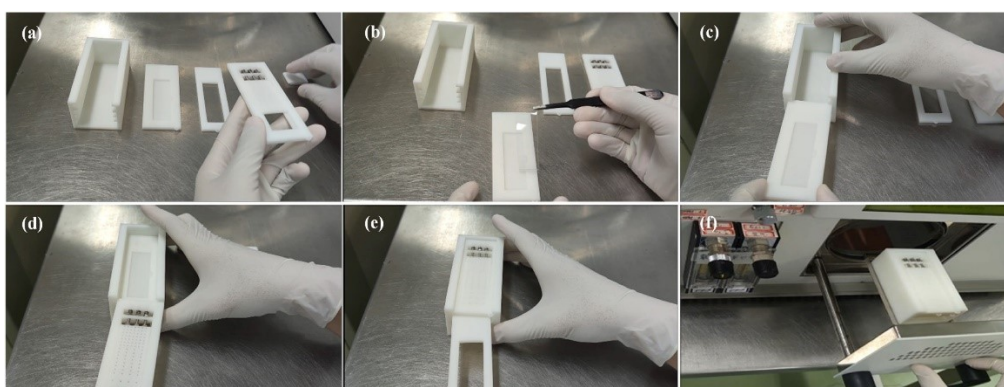


Fig. S1 The CGPM process. (a) Insert the mask into the mask fixture in sequence. (b) Put the material into the microdevice fixture. (c) Insert the microdevice fixture into the holder. (d) Insert the mask fixture into the holder. (e) Insert the support plate into the holder. (f) Put the CGPM device into the solid-state RF plasma barrel reactor.

The discharge plasma chemistry can be simplified to a chemical reaction system consisting of 3 substances and 2 reactions, as shown in Table S1 and Table S2. For ions, a local field approximation was used to calculate the ion temperature, and a look-up table was used to obtain the ion mobility. Electron mobility and other transfer properties were calculated automatically based on a list of electron collision reactions. It is assumed that the loss of ions at the wall was caused by migration alone.

Tab. S1 Electron impact reactions in the plasma simulation system and setting of simulation parameters

Reaction	Equation	Type	Energy loss
1	$e+\text{He} \Rightarrow e+\text{He}$	Flexible	0
2	$e+\text{He} \Rightarrow e+\text{Hes}$	Incentive	19.8
3	$e+\text{He} \Rightarrow 2e+(\text{He}^+)$	ionized	24.6

*where e is the electron, He is the helium atom, Hes is the excited state of helium, and (He⁺) is the ionic state of helium

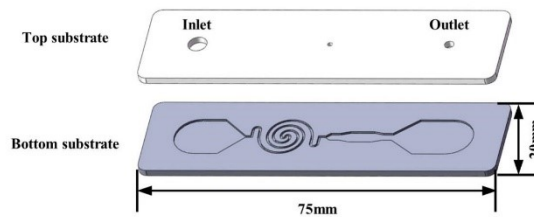
Tab. S2 Heavy species reactions in the plasma simulation system and setting of simulation parameters

Reaction	Equation	Adhesion coefficient	Secondary emission factor	Secondary electron average energy
1	$(\text{He}^+) \Rightarrow \text{He}$	1	0.07	5.8
2	$\text{Hes} \Rightarrow \text{He}$	1	0.1	5.8

The grid-independent test was carried out for the model with the mesh number of 4292, 5942, 8398, 19244, 31406, 44298, 70898 and hole side length of 2mm. When the number of grids is 31406, and the number of grids is increased, the electron density is almost unchanged. Therefore, in order to improve computational efficiency, the total number of grids is set at 31406.

Tab. S3 The comparison of plasma density with different numbers of meshes

No.	Elements	Nodes	Plasma density(m ³)
1	4292	2217	3.49×10^{14}
2	5942	3042	3.53×10^{14}
3	8398	4270	3.89×10^{14}
4	19244	9693	4.42×10^{14}
5	31406	15774	4.61×10^{14}
6	44298	22220	4.64×10^{14}
7	70898	35520	4.58×10^{14}

**Fig. S2** The shape of the integrated POCT microfluidic device

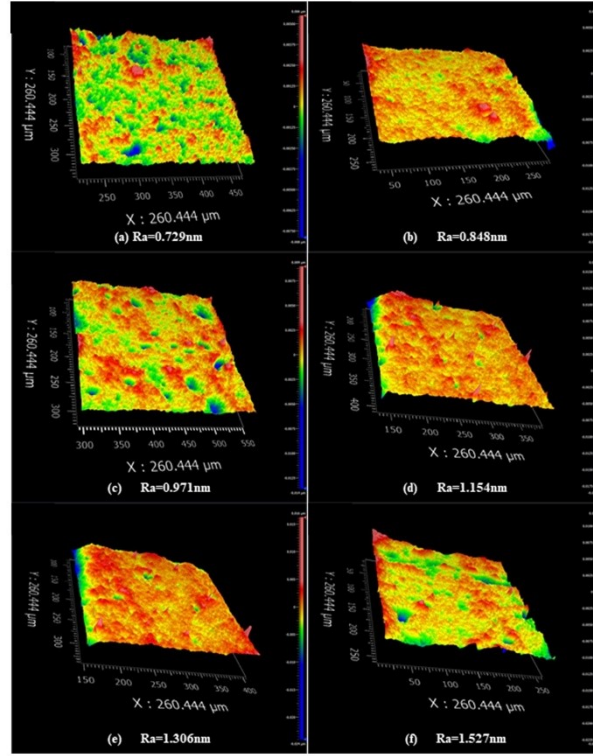


Fig. S3 Surface morphology investigation of the modified surface. Surface morphology by using different masks: (a) with mask A. (b) with mask B. (c) with mask C. (d) with mask D. (e) with mask E. (f) with mask F

The fluid in the microchannel of PMD is driven by capillary forces, so the flow rate is determined by the surface wettability of the PMD, the viscosity of the fluid, the resistance to flow, and the capillary pressure. It can be calculated by the equation (1):

$$Q = \frac{1\Delta P}{\eta R_F} \#(1)$$

where η is the viscosity of the liquid, ΔP is the pressure difference before and after the liquid, which can be taken as the capillary pressure P_c in the PMD, and R_F is the resistance to flow along the flow path. The P_c in the channel can be calculated from the equation (2):

$$P_c = -\gamma \left[\left(\frac{\cos\alpha_t + \cos\alpha_b}{H} \right) + \left(\frac{\cos\alpha_l + \cos\alpha_r}{W} \right) \right] \#(2)$$

Where γ is the surface tension of the liquid and α_t , α_b , α_l , α_r are the contact angles at the top, bottom left, and right walls of the channel. The flow resistance R_F can be calculated from the equation (3):

$$R_F = \left[\frac{1}{12} \left(1 + \frac{5H}{6W} \right) \frac{HWR_H^2}{L} \right]^{-1} \#(3)$$

Where h is the depth of the microchannel, w is the width, L is the length and R_H is the hydrodynamic radius of the microchannel, which can be calculated as the ratio of the cross-sectional area to half the wet perimeter:

$$R_H = \frac{A}{P/2} = \frac{HW}{H+W} \quad (4)$$

The above theoretical analysis shows that the flow rate in the microchannel is related to the wettability and geometry of the microchannel. Furthermore, the calculated flow rates at different contact angles are shown in the Fig. S3:

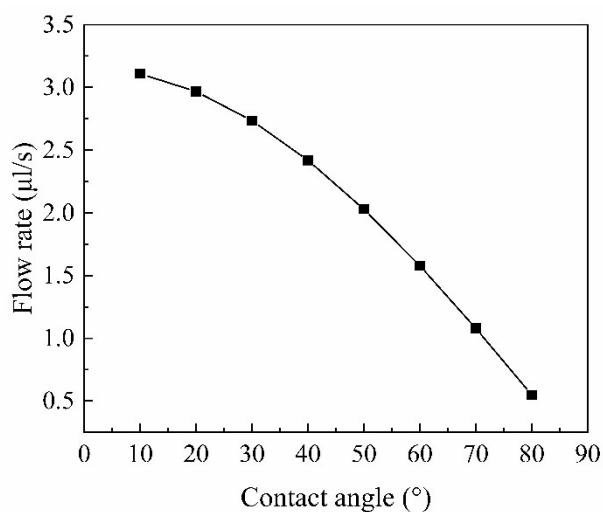


Fig. S3 Relationship between contact Angle and volume flow rate in a microchannel with a height of 80um and a width of 2mm

Tab. S4 Repeatability testing for D-dimer assays

Concentration(ng/ml)	Mean relative fluorescence intensity(a.u.)	Absolute deviation	Relative Error(%)
1	21.03	1.95	9.3
10	31.74	2.78	8.8
100	51.86	3.04	5.9
500	75.32	2.28	3.0
1000	80.94	2.54	3.1